CellPress
OPEN ACCESS

Trends in
Chemistry

Review

Cation-coupled chloride cotransporters: chemical insights and disease implications

Corinne Portioli,[1,2] Manuel José Ruiz Munevar,[2] Marco De Vivo,[2,4,*] and Laura Cancedda[1,3,4,*]

Cation-coupled chloride cotransporters (CCCs) modulate the transport of sodium and/or potassium cations coupled with chloride anions across the cell membrane. CCCs thus help regulate intracellular ionic concentration and consequent cell volume homeostasis. This has been largely exploited in the past to develop diuretic drugs that act on CCCs expressed in the kidney. However, a growing wealth of evidence has demonstrated that CCCs are also critically involved in a great variety of other pathologies, motivating most recent drug discovery programs targeting CCCs. Here, we examine the structure–function relationship of CCCs. By linking recent high-resolution cryogenic electron microscopy (cryo-EM) data with older biochemical/functional studies on CCCs, we discuss the mechanistic insights and opportunities to design selective CCC modulators to treat diverse pathologies.

Highlights

The structural topology and function of all cation-coupled chloride cotransporters (CCCs) have been continuously investigated over the past 40 years, with great progress also thanks to the recent cryogenic electron microscopy (cryo-EM) resolution of the structures of five CCCs. In particular, such studies have clarified the structure–function relationship for the Na-K-Cl cotransporter NKCC1 and K-Cl cotransporters KCC1–4.

The constantly growing evidence of the crucial involvement of CCCs in physiological and various pathological conditions, as well as the evidence of their wide expression in diverse body tissues, has promoted CCCs as targets for the discovery and development of new, safer, and more selective/effective drugs for a plethora of pathologies.

Post-translational modification anchor points on the structure of CCCs may offer alternative strategies for small molecule drug discovery.

Cation-coupled chloride cotransporters (CCCs): from structure to function and modulation

CCCs are proteins (~130 kDa) of the subfamily of solute carrier **transporters** (see Glossary) 12 (SLC12) that modulate transport of sodium and/or potassium cations (Na^+, K^+) and chloride anions (Cl^-) across the cell membrane (Figure 1A). In humans, there are seven known electroneutral CCCs: the Na^+–Cl^- cotransporter NCC, the Na^+-K^+-Cl^- cotransporters NKCC1 and NKCC2, and the K^+-Cl^- cotransporters KCC1, KCC2, KCC3, and KCC4 (Figure 1B) [1]. NCC and NKCC2 are expressed predominantly in the kidney [2]. NKCC1, KCC1, KCC3, and KCC4 are expressed throughout the body. KCC2 is expressed specifically in neurons [3]. CCCs are involved in physiological processes, including salt absorption and secretion, cell volume regulation, and intracellular Cl^- concentration setting [1,4]. As such, CCCs are primarily implicated in blood pressure regulation, cardiovascular and brain physiopathology, and diuresis, and are also associated with hearing and tumoral diseases (Figure 1C,D).

Structure–function relationships

CCCs mainly form homodimers, although multimeric states have been described in functional assays for N(K)CCs and KCCs [5–7]. Monomers for each of the CCC family members are characterized by a well-conserved transmembrane (TM) domain formed by 12 TM helices, one *N*-glycosylated extracellular (EC) domain, and, on the cytosolic side, the amino-terminal (NT) and the large carboxy-terminal (CT) domains (Figure 1A). All SLC12-CCC members share the same TM protein fold of the leucine transporter (LeuT [8], Box 1). The EC domain is characterized by a connecting loop between TM7 and TM8 in Na^+-dependent CCCs, whereas Na^+-independent CCCs have a longer loop between TM5 and TM6. The NT and EC domains are variable in amino acid length, much shorter than the CT domain, and poorly conserved among the CCC members. The EC domains contain glycosylation sites, whereas the intracellular domains contain phosphorylation sites to modulate CCC function (Figure 1A) [9]. Molecular heterogeneity is also provided by multiple CCC isoforms, generated by alternative splicing and alternative promoter usage [10].

[1]Brain Development and Disease Laboratory, Istituto Italiano di Tecnologia (IIT), Via Morego 30, 16163 Genoa, Italy
[2]Laboratory of Molecular Modeling and Drug Discovery, IIT, Via Morego, 30 16163 Genoa, Italy
[3]Dulbecco Telethon Institute, Via Varese 16b, 00185 Rome, Italy
[4]These authors contributed equally to this work

*Correspondence:
marco.devivo@iit.it (M. De Vivo) and
laura.cancedda@iit.it (L. Cancedda).

Many functional and mutagenesis studies have detected and measured ion/ligand binding and ion transport [11], indicating that the variation of residues in the TM domains or truncation of the CT domain can compromise ion affinity and transport activity [12,13]. In particular, the CT domain plays a key role in CCC assembly [5,6,14–16], as demonstrated by cell and chemical biology studies on NCC oligomerization in glycosylated monomers and multimers. For example, mistargeting to the plasma membrane is a possible cause of degradation of NCC chimeras formed by coexpression of wild type (WT)-NCC and CT domain mutant subunits [16]. Moreover, in the prokaryotic CCC homolog, the CT domain dimer-interface shows small and hydrophilic buried areas that can be disrupted by point **mutations** and regulate dimerization [14]. The complex structure of CCCs allows formation of discrete ion-**binding sites** nested within the TM domains, although ion selectivity and stoichiometry can differ among NCC, NKCCs, and KCCs [17]. Ion translocation occurs via the alternating access model, which involves switching between an inward-open (IO) ↔ outward-open (OO) **conformational state** that exposes the ion-binding sites to either side of the membrane (Box 1) [18,19].

New structural insights from recent cryo-EM structures

Five CCC members have been resolved with **cryo-EM** (i.e., NKCC1 and KCC1-4 [20–26]), confirming the dimeric organization of CCCs, with the exception of mouse (*m)*KCC4 resolved as a monomer [27]. The first high-resolution structures of zebrafish [*Danio rerio* (*Dr*)] NKCC1 [20] and human (*h)*KCC1 [21] were reported in 2019. In 2020–2021, six independent studies reported new structures of *h*NKCC1, *m*KCC2, and *h*KCC2-4 transporters, alone or in complex with inhibitors (Table 1 and Box 2) [20–28]. These structural data confirmed the predicted LeuT structural fold with a large ordered and glycosylated loop in the EC domain and two cytosolic domains (NT and CT) with numerous phosphorylation sites. Moreover, these data revealed that TM11 and TM12 form the dimerization interface through an inverted V-shaped structure (helix-turn-helix), while the TM12-scissor helix connects the TM with the CT domain. The dimerization seems also to be aided by cell membrane lipids at the interface region [26].

The specific conformation of the resolved transporters has been crucial to determine what structural features modulate the IO ↔ OO conformational state switch. This is central to understanding the mechanism for ion permeation in CCCs. In particular, some of the solved IO conformation structures of the CCC dimers (i.e., *Dr*NKCC1, *h*KCC1, *m*KCC2, *h*KCC2a-b, *h*KCC3a-b, *h*KCC4a [20,23–26]) showed the CT dimeric domain in the full-length molecular assembly for the first time. These structures also revealed that the CT domain of one **protomer** is located under the TM domain of the other protomer, creating a domain-swap configuration that stabilizes the dimerization. For *h*KCC2-4, the dimeric structures of the CT domains are stabilized also by hydrophobic interaction among the scissor helix and other structural CT features [24]. Although resembling the architecture of the dimeric prokaryotic CCC domain structure [14], the CT domain in *Dr*NKCC1 is slightly tilted with respect to the TM region, when observed perpendicular to the membrane. Moreover, in *h*KCC2 and *h*KCC3, the CT domain is rotated clockwise by 70° as seen from the intracellular side, compared with *Dr*NKCC1 [25]. The CT domain of *h*KCC2 and *h*KCC4 weakly interacts with the TM domain (at the junction between TM12 and the scissor helix) through hydrogen bonds [24].

An NT domain peptide was also resolved in the *m*KCC2, *h*KCC2a-b, *h*KCC3b, and *h*KCC4a structures, where it sterically closes the cytosolic vestibule and blocks transport activity [24–26]. Deletion or mutation of the NT domains in KCC2b and KCC3b enhances transport activity [24–26], which supports the role of the NT domain as an autoinhibitory element. This closed (autoinhibitory) state is well characterized in the KCC2a and KCC4a structures, where an NT domain peptide is

Glossary

Binding site: a protein pocket that can bind physiological (endogenous) or exogenous compounds that may act as substrates and/or modulators. Its determination is crucial for drug design.
Conformational state: the spatial arrangement of the atoms and chemical groups forming a molecule. The conformational state is characterized by energetic and thermodynamic properties. Buffer pH, temperature, buffer composition, and the presence of ligands/cofactors can induce a change in the conformational state of a molecule.
Cryo-EM: a technique that uses cryogenic temperatures to cool and embed protein samples in a vitrified layer of water. In cryo-EM experiments, the samples are spotted on grids and plunge-frozen in liquid ethane, before being observed with the transmission electron microscope. This approach for macromolecular structure determination, alternative to classical structural resolution, does not require sample crystallization.
Mutation: an alteration in the nucleotide sequence of a genome that could be missense, deletion, nonsense, frameshift, or altered splice site. Mutations can lead to the modification of one or more amino acids to another one, in the protein structure or truncated proteins; alternatively, mutations can be silent, when there are no changes in the amino acid residues in the protein.
Protomer: structural unit involved in a multi/oligomeric state.
Transporter: membrane protein that forms a translocation pathway, allowing the movement of molecules (ions, nutrients, ligands, drugs) across the plasma membrane of a cell.

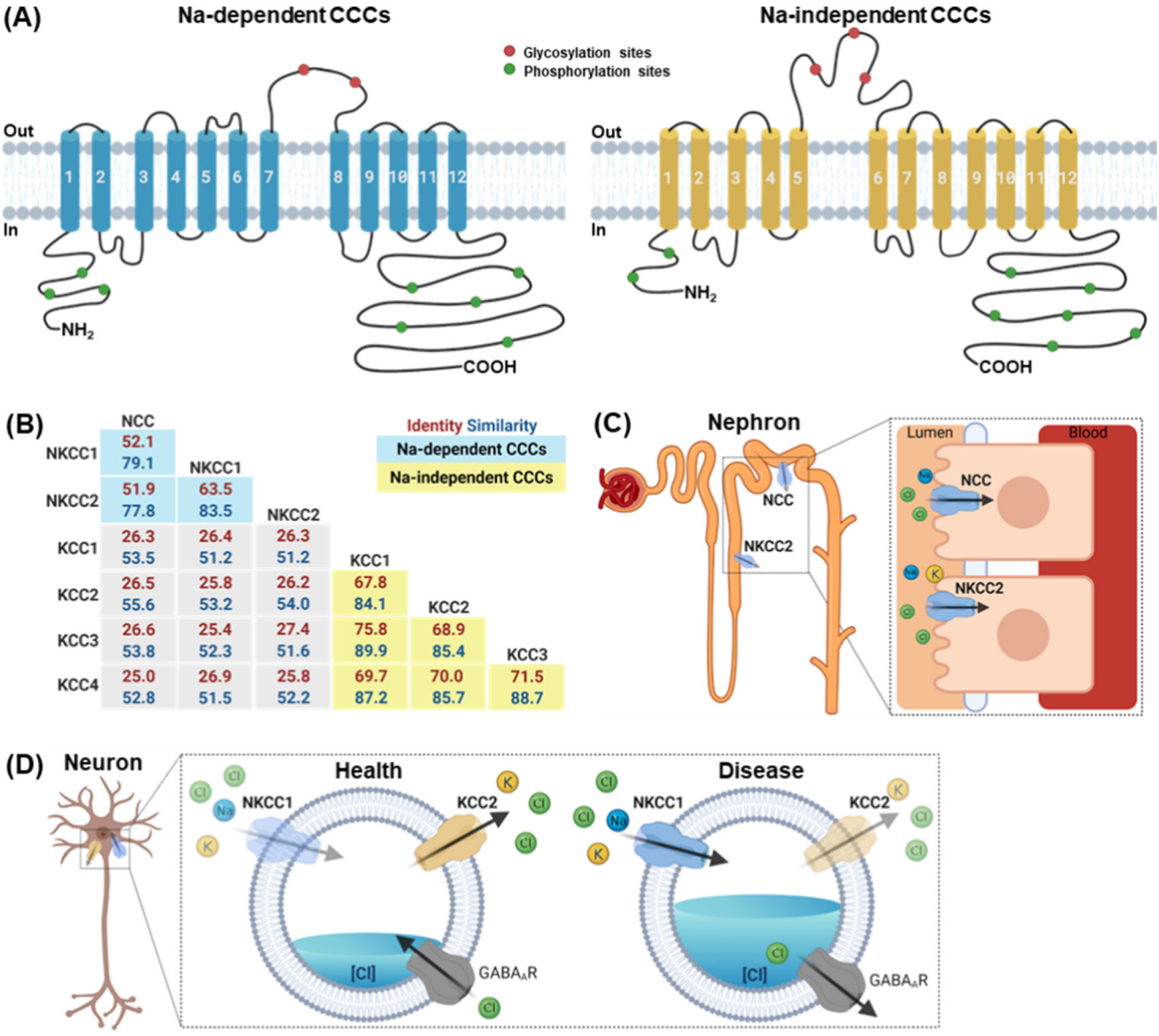

Trends in Chemistry

Figure 1. Cation-coupled chloride cotransporter (CCC) structures and functions. (A) Schematic representation of CCC topology based on LeuT homology amino acid sequence alignments and structural studies. CCCs are characterized by 12 helices in the transmembrane (TM) domain and a large extracellular (EC) domain. The EC domain is formed mainly by a large loop between TM7 and TM8 for Na^+-dependent CCCs, and TM5 and TM6 for Na^+-independent CCCs. An N terminal (NT) domain and a large C terminal (CT) domain are located intracellularly for all CCCs. Within the extra- and intracellular domains there are key residues that can modulate the activity of the transporter via phosphorylation (green dots) or glycosylation (red dots). (B) Homologies (expressed as percentage of identity, residues that match between two protein amino acid sequences, and similarity, residues with similar physico-chemical properties) among the protein amino acid sequences of human Na^+-dependent CCCs (NCC isoform 1, NKCC1 isoform 1, NKCC2 isoform a) and human Na^+-independent CCCs (KCC1 isoform 1, KCC2 isoform 1 or a, KCC3 isoform 1 or a, KCC4 isoform 1). The sequence alignment was performed using pairwise sequence alignment with LALIGN software (EMBL-EBI). (C) Schematic representation of the functional role of Na^+-Cl^- importer NCC and Na^+-K^+-Cl^- importer NKCC2 in a kidney nephron. (D) Schematic representation of the functional role of Na^+-dependent Na^+-K^+-Cl^- importer NKCC1 and Na^+-independent K^+-Cl^- exporter KCC2 in a neuronal cell in health and diseases. Arrows indicate the direction of the ionic flux. All representations were created with BioRender.com.

bound mainly though hydrogen bond interactions with TM1a, TM5, TM6b, and TM8. Notably, residues in the central portion of the NT domain are conserved among KCCs, suggesting a similar autoinhibitory mechanism [24,26]. Comparison of the full-length *Dr*NKCC1 structure with the NT

domain truncated structure indicates only minor structural adjustments between the TM and CT domains, with the proteins maintaining a similar overall conformation [20].

Finally, the EC domain was resolved in all the recent cryo-EM structures. In the first *h*KCC1 structure (solved in the IO conformation), the two EC domains interact with one another, forming a dimeric closing cap towards the EC side. This seals the cavity formed by the TM domains [21]. In *m*KCC2, *m*KCC4, and *h*KCC2a, the EC gate is sealed by salt-bridge Lys(Arg)-Glu(Asp) interactions, formed between residues along the TM7-TM8 linker, TM1, TM3, and TM10 domains interface [24,26,27]. Based on homology modeling and sequence alignment [1], NCC and NKCC2, the structures of which are not yet solved, are expected to have the same structural architecture of the two EC domains and overall dimeric closing cap mechanism.

Ion-binding sites

Of the new CCC structures solved in the IO conformation, some contained ions inside the TM domain (Table 1 and Box 1) [20,21,24,25,27]. Such ion-binding sites were tested also through molecular dynamics (MD) simulations, even based on structures originally solved without ions [20,26]. Overall, this confirmed previous homology modeling, sequence alignment, and biochemical studies, which suggested plausible ion-binding sites at the TM domain [1,11]. These ion-binding sites are surrounded by the TM3 and the two discontinuous helices TM1 and TM6, connected by two flexible and conserved Gly residues as linkers (e.g., G301, TM1a-TM1b and G500, TM6a-TM6b, in *h*NKCC1) [22,26]. In NKCC1, the binding sites can be loaded from the EC gates through three potential entryways (one each for Na^+, K^+, and Cl^- ions). In NKCC1 IO structures, the gates have been captured either occluded (sealed via salt bridges) or open, suggesting a key role of TM1, TM3, TM5, TM6, and TM8 in EC-gating modulation [20,22]. Three exit pathways to the cytoplasm were proposed (possibly one each for Na^+, K^+, and Cl^- ions) [22]. A key gating role is also played by hydrogen bonds involving R294 on TM1 and Q435 on TM5 of *h*NKCC1. This residue, conserved in all Na^+-dependent CCCs, is proposed to stabilize the open state of the intracellular gate [22,26]. The mechanism for ion permeation implies that Na^+ binds first, followed by one Cl^- ion, then the K^+ ion, and finally a second Cl^- ion [18]. Ions would then be released into the intracellular side in the same order, likely allowing the passage of some water molecules [26,29]. Nevertheless, this still needs to be proven, since current structures lack the resolution to clearly detect bound water molecules in the ion pathway.

The new CCC structures revealed that Na^+ coordination is mediated by conserved Ser residues on TM8 (S538-S539 in *Dr*NKCC1, S613-S614 in *h*NKCC1) [20,22]. Notably, these serines (and/or threonines) are highly conserved among CCC transporters, with a similar TM fold and in line with what has been observed in LeuT and neurotransmitter/sodium symporter (NSS) family homolog

Box 1. Mechanism for ion transportation

CCC ion transporters are characterized by a structural topology that was first described for LeuT [in both outward-open (OO) and inward-open (IO) states, substrate free] [31], a bacterial (*Aquifex aeolicus*) amino acid/Na^+ symporter and member of the amino acid-polyamine-organocation (APC) transporter superfamily [8]. A number of APC transporters, all adopting a similar LeuT fold, have been solved: the Na^+/hydantoin transporter, Mhp1 [116], amino acid antiporter, AdiC [117], Na^+/betaine symporter, BetP [118], Na^+-independent amino acid transporter, ApcT [119], Na^+/galactose symporter, vSGLT [120], carnitine transporter, CaiT [121], and sialic acid transporter, SiaT (Figure IA) [122]. The LeuT fold is characterized by a pseudo twofold symmetry, with two five-helix repeats (TM1–5 and TM6–10) orientated in an inverted architecture along the vertical axis, with a central binding cavity for Na^+ ions and leucine. Importantly, knowledge of the structure–function relationship of LeuT guided mutagenesis, cell-based assays, and *in vitro* studies with radiolabeled substrates of CCCs [8,31]. LeuT transporter functions through the rocking-bundle alternating-access mechanism, which diversifies transporters from channels. This involves a multistate isomerization with OO, ligand bound/occluded, and IO states. These allow the substrate to cross the membrane [30]. A similar mechanism has been hypothesized also for CCCs. For example, in Na^+-dependent CCCs, the access model starts with ions that first bind extracellularly in an OO (empty) state of the transporter. This triggers an initial conformational state change of the transporter toward a loaded occluded state. Then, the transporter gradually moves into an IO conformation. This OO → IO conformational state transition releases the ions into the cell, with the transporter then returning to an OO conformation. In this latter conformation, the transporter is ready to restart the stepwise mechanism for ion internalization (Figure IB,C). For all CCCs, what remains unclear is the exact dynamic mechanism and trigger for state interconversion.

(A)

APC transporter		Organism	State	Substrate	Detergent	Res (Å)	PDB	Refs
AdiC	L-arginine-agmatine transporter	*Salmonella enterica* *Salmonella typhimurium*	OO	–	DDM	3.2	3NCY	[117]
ApcT	Na-independent H-coupled amino acid transporter	*Methanocaldococcus jannaschii*	IFO	–	OTG	2.32	3GIA	[119]
BetP	Na/betaine symporter	*Corynebacterium glutamicum*	OO, OFO, IOB	Choline	DDM	3.25	4DOJ	[118]
			O, OB, IOB	Betaine		3.1	4AIN	
CaiT	L-carnitine/butyrobetaine transporter	*Proteus mirabilis*	IO	Betaine	C5	2.29	2WSW	[121]
		Escherichia coli				3.5	2WSX	
LeuT	Na/Cl-dependent neurotransmitter transporter homolog	*Aquifex aeolicus*	OFO	Leu, 2Na, 1Cl	DDM	1.65	2A65	[8,31]
			OO	2Na	OTG	3.1	3TT1	
			IO	–		3.22	3TT3	
Mhp1	Na/benzyl-hydantoin transporter	*Microbacterium liquefaciens*	OO	Na, Hg	DDM	2.85	2JLN	[116]
			IO	–		3.8	2X79	
SiaT	Na-coupled sialic acid transporter	*P. mirabilis*	OO	Neu5Ac, 2Na	DDM	1.95	5NV9	[122]
vSGLT	Na-galactose transporter	*Vibrio parahaemolyticus*	IFO	Galactose, Na	DDM	2.7	3DH4	[120]

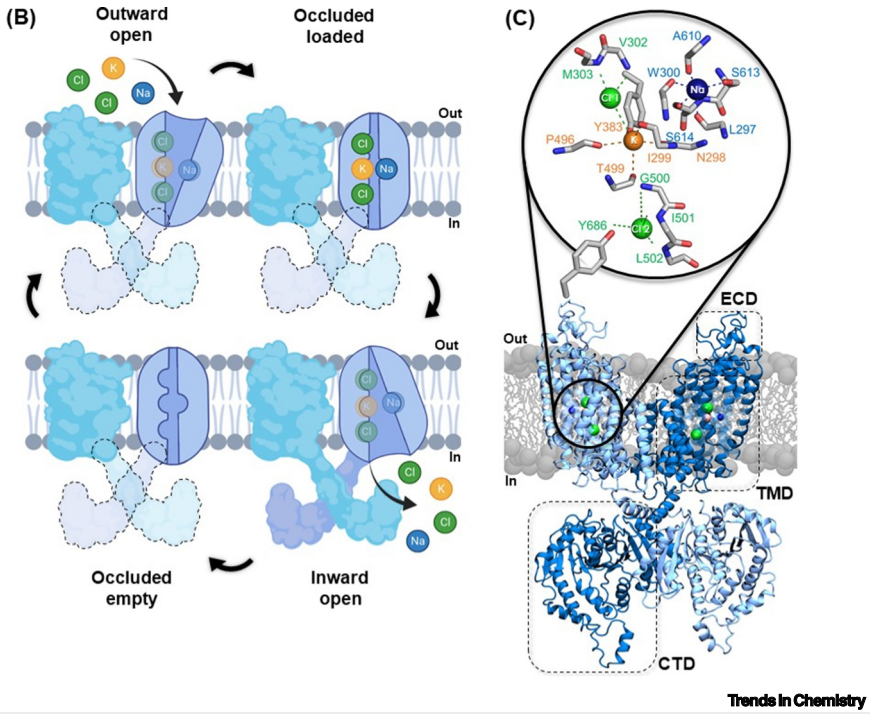

Figure I. Mechanism for ion transportation in cation-coupled chloride cotransporters (CCCs). (A) Table summarizing all the bacterial amino acid-polyamine-organocation (APC) transporters that have been solved using X-ray crystallography. The APC transporters were solved in different conformational states of the transmembrane (TM) domain: inward-open (IO), outward-open (OO), inward-open ligand bound (IOB), inward facing occluded (IFO), outward facing occluded (OFO), and occluded bound (OB). (B) Schematic representation of the different states that Na^+-dependent CCCs adopt to transfer ions across the cell membrane. The C terminal (CT) domain is shown for completeness of information, although represented as transparent for states in which its exact conformation and position are not known, yet. A similar mechanism of ion transport (although in the opposite direction) has been hypothesized for Na^+-independent CCCs. Representation was created with BioRender.com. (C) Model of NKCC1 structure obtained by merging the TM domain of *h*NKCC1 (PDB code: 6PZT), with bound ions (Cl^- ions are in green, K^+ in orange, and Na^+ in blue), and the CT domain of the *Dr*NKCC1 (PDB code: 6NPL), all solved by cryogenic electron microscopy. Each monomer is formed by extracellular (EC)-TM-CT domains. In this figure, one monomer is depicted in light blue (left) and the other in dark blue (right). In this representation, the right monomer is in front of the left monomer, which remains behind in the domain swap configuration. The magnified area shows the residues (in *h*NKCC1) that form the ionic binding sites. We performed the merging using the software Visual Molecular Dynamics. Abbreviations: CTD, C terminal domain; DDM, *n*-dodecyl β-D-maltoside; ECD, extracellular domain; OTG, octylthioglucoside; PDB, Protein Data Bank; TMD, transmembrane domain.

Table 1. High resolution cryo-EM structures[a]

CCC isoform		Construct	Resolution (Å)	Ions	Conformation	Expression system	Buffer	PDB	Refs
NKCC1		Zebrafish: full length & NT domain truncated	2.9 (TM + CT domains)	2Cl, 1K	IO	Sf9 using Bacmid system	20 mM Tris-HCl pH 8, 200 mM KCl, 200 mM NaCl, 0.06% digitonin	6NPL	[20]
			2.9 (TM domain)	2Cl, 1K				6NPH	
			3.6 (TM domain)	–				6NPK	
			3.8 (CT domain)	–				6NPJ	
	a	255–278 (NT domain del) & 941–1000 (CT domain del), K289N & G351R	3.46 (TM domain)	–	IO	HEK 293S GnTI$^-$ using BacMam system	20 mM Hepes pH 7.4, 150 mM NaCl, 0.5 mM, TCEP, 0.025 mM LMNG, 0.005 mM CHS	6PZT	[22]
		Full length	3.5 (TM domain)	–	IO	HEK 293F using BacMam system	20 mM Hepes pH 7.4,150 mM NaCl, digitonin	7D10	[26]
KCC1	a	Full length	2.9 (TM domain)	2Cl, 1K	IO	HEK 293F using BacMam system	20 mM Tris pH 8, 150 mM KCl, 0.06% GDN	6KKR	[21]
			2.9 (TM domain)	2Cl, 1K			20 mM Tris pH 8, 150 mM KCl, lipid nanodiscs	6KKT	
			3.5 (TM domain)	1Cl			20 mM Tris pH 8, 150 mM NaCl, 0.06% GDN	6KKU	
		Full length	3.25 (TM + CT domains)	1K	IO	HEK 293S GnTI using BacMam system	20 mM Hepes pH 7.4, 150 mM KCl, 0.5 mM TCEP, 0.025 mM LMNG, 0.005 mM CHS	NA	[23]
		Full length + VU0463271	3.63 (TM domain)	–	OO		20 mM Hepes pH 7.4, 150 mM NaCl, 0.5 mM TCEP, 0.025 mM LMNG, 0.005 mM CHS, 0.025 mM VU0463271	NA	
KCC2	a	Full length	17.4	–		HEK Expi293F transfected with DNA & PEIMax	PBS 1X, 1.5 mM CALX-R3, 0.6 mM DDM	NA	[15]
		Full length	3.4 (~NT + TM + CT domains)	2Cl, 1K	IO	HEK 293F using BacMam system	30 mM Tris-HCl pH 8, 150 mM KCl, 0.02% GDN	7D8Z	[24]
		Mouse, full length	3.8 (~NT + TM + CT domains)	–	IO	HEK 293F using BacMam system	20 mM Hepes pH 7.4, 150 mM NaCl, 0.1% digitonin	7D14	[26]
	b	Full length	3.2 (~NT + TM + CT domains)	1Cl, 1K	IO	HEK 293F transfected with DNA & PEIs	25 mM Tris pH 8, 150 mM NaCl, 0.02% GDN	6M23	[25,28]
KCC3	a	Full length	3.6 (TM + CT domains)	–	IO	HEK 293F using BacMam system	30 mM Tris-HCl pH 8, 150 mM KCl, 0.02% GDN	7D90	[24]
	b	Full length	3.3 (TM + CT domains), 3.1 (TM domain) - 2.9 (CT domain)	–	IO	HEK 293F transfected with DNA & PEIs	25 mM Tris pH 8, 150 mM NaCl, 0.02% GDN	6M1Y	[25,28]

(continued on next page)

Table 1. (continued)

CCC isoform		Construct	Resolution (Å)	Ions	Conformation	Expression system	Buffer	PDB	Refs
		Full length + DIOA	2.5 (TM + CT domains)	2Cl, 1K				6M22	
		Full length deP mutant S45A/T940V/T997V	3.2 (TM + CT domains)	–				NA	
		Full length P mutant S45E/T940E/T997E	2.9 (TM + CT domains)	–				NA	
		Full length S45D/T940D/T997D	3.76	–				6Y5R	
		Full length S45D/T940D/T997D	4.08	–				6Y5V	
KCC4		Mouse, full length	3.65 (TM domain)	1Cl, 1K	IO	Sf9 using Bacmid system	20 mM Tris pH 8, 150 mM KCl, 1 mM EDTA, 0.025% DDM, 0.0025% CHS	6UKN	[27]
	a	Full length	2.9 (~NT + TM + CT domains)	2Cl, 1K	IO	HEK 293F using BacMam system	30 mM Tris-HCl pH 8, 150 mM KCl, 0.02% GDN	7D99	[24]

[a]Abbreviations: CALX-R3, calixarene-base detergent; CHS, cholesteryl hemisuccinate; DDM, *n*-dodecyl β-D-maltoside; GDN, glyco-diosgenin; LMNG, lauryl maltose neopentyl glycol; TCEP, tris(2-carboxyethyl)phosphine; NA, PDB not available (yet).

structures [8,30,31]. Interestingly, in KCCs (activity of which does not require Na^+), the conserved Ser residues in TM8 are replaced by one Cys and one Gly [20].

In the *Dr*NKCC1 structure, the K^+ ion binds to residues on the discontinuous helices TM1 (N220 and I221), TM6 (T420 and P417), and to a highly conserved Tyr along TM3 (Y305 in *Dr*NKCC1 and Y383 in *h*NKCC1) [20,22,26], confirming previous studies [13]. Interestingly, Y383 is conserved in NKCCs and KCCs, but not in NCC, strengthening the notion that it may be required for K^+ transport. In addition, kinetic experiments in NKCC2 suggested the involvement of P254 and A267 in TM3 and T235 in TM2 for K^+ binding [5,32]. In *h*KCC1 (Y216), *h*KCC2a (Y218), and *h*KCC4a (Y216) structures, a Tyr residue contributes to specific K^+ binding [21,24,26]. Mutations of Y216, T432, Y589, and S430 reduce or abolish KCC1 function [21]. Notably, K^+ transport activity is reduced by mutation of residues R140, K485, and F486, which disrupts the EC–TM domain interaction network in *m*KCC4. This is because this region is involved in the loading of K^+ between TM1, TM3, and TM6 (and Cl^- between TM6 and TM10) [27].

Finally, the *Dr*NKCC1 cryo-EM structure and MD simulations suggested two Cl^- binding sites (Cl1 and Cl2) above and below the K^+ binding site, in a region between TM1, TM6, and TM10. In MD simulations, Cl^- ions transiently bind to such solvent-accessible sites of the transporter [20,26]. Simulations of *Dr*NKCC1 suggested that the K^+ ion is also involved in Cl^- coordination, together with Y454 (in Cl1) and Y611 (in Cl2). Mutations of any of these residues reduce or abolish the Cl^- transport [20]. In KCC1, Cl^- in Cl1 is coordinated by G134, V135, I136, S430, and the K^+ ion, whereas Cl^- in Cl2 is coordinated by G433, I434, M435, and Y589 [21]. Although Cl^- in Cl1 was not resolved in *m*KCC4, mutation of Y466, which is equivalent to Y454 in *Dr*NKCC1, reduces transport activity [27]. Interestingly, KCC4 transport activity is decreased by mutation of the CCC-conserved residues Y589 in TM10 and Y216 in TM3, which coordinate Cl^- and K^+, respectively [27].

Modulation of CCC activity by post-translational modifications

There are key phosphorylation residues in the NT and CT domains that modulate transporter expression, trafficking, activity, and oligomer/cluster formation in lipid rafts [33–37] (Table 2). The structure determination of both WT and dephosphorylation-mimic cryo-EM KCC3b structures allowed identification of mutations that mimic the effect of (de)phosphorylation. In KCC3b, T997 phosphorylation might be involved in maintaining the IO conformation by stabilizing the TM10-11 loop [28]. Such (de)phosphorylation events in CCCs often involve the 'With No Lysine' (WNK) Ser–Thr kinases. For example, WNK1 and WNK3 enhance NCC function by increasing its expression, whereas WNK4 inhibits NCC function [38,39]. Interestingly, GABAergic transmission is modulated by increased WNK1 phosphorylation, which promotes NKCC1 phosphorylation/activation and KCC2 phosphorylation/inactivation in neurons [36,40]. Moreover, WNK1 and WNK3 also activate NKCC2 through phosphorylation at NT domain residues [41,42]. Mutations of T96, T101, and T111 residues inhibit NKCC2 phosphorylation and activity in low Cl^- hypotonic stress, which normally activates NKCC2 [41]. In *h*KCC3, key residues in the NT and CT domains are highly phosphorylated in isotonic conditions via WNK1 and WNK3, which lead to physiological inactivation of the transporter [34,43,44]. Mutation of these Thr residues to Ala resulted in constitutively active cotransport, suggesting that preventing phosphorylation may increase the activity [34]. Finally, the WNK kinases can also affect CCC regulation via the downstream kinase Ste20-related proline-alanine-rich kinase (SPAK)/oxidative-stress response 1 (OSR1) and the protein kinase A and C (PKA and PKC) [37,42–47]. These additional players can form direct contacts with CCCs. This is the case for a 92-residue motif on the SPAK/OSR1 CT domain, which interacts with the NT domain of NKCC1 or the CT domain in KCC3 (and the motif RFXV in WNK1 and WKNK4) [43,46]. Interestingly, WNK3 activation by the WNK3-SPAK complex (or alone) enhances *h*NKCC1 activity through phosphorylation of T212 and T217 in concert with inhibitory KCC3 phosphorylation [43].

The glycosylation sites in CCCs are conserved EC domain residues in the loop between TM7 and TM8 in NCC and NKCCs, and in the loop between TM5 and TM6 in KCCs [1]. For example, the recent *h*KCC1 cryo-EM structure revealed two *N*-linked glycosylated residues in the long EC loop. This loop has six *N*-linked glycosylation sites in KCC2 [48]. Glycosylation controls the correct folding and membrane localization of CCCs, preventing internalization and degradation of the transporter (Table 2) [49]. For example, mutation of glycosylation sites at the EC domain

Box 2. Small-molecule binding to, and protein amino acid-sequence mutations in, CCCs linked to human disorders

The recently resolved CCCs are all in IO conformations only, but KCC1 was also resolved in an OO conformation. Moreover, KCC3 structure was resolved in complex with the inhibitor dihydroindenyl-oxy acetic acid (DIOA) and KCC1 was resolved in complex with the inhibitor VU0463271. The KCC3-DIOA complex showed that DIOA interacts with specific residues in the TM10-11 loop (R617) and TM12 (K664) in the central cleft between the two monomers of KCC3 (Figure IA) [28]. Interestingly, these residues are conserved in KCCs, but not in NKCCs. The KCC1-VU0463271 complex was resolved in the OO conformation [23]. Here, the drug fits a pocket formed by TM1b, TM6a, TM3, and TM10. In particular, VU0463271 hampers a salt bridge between R140 and E222, involved in the outer gate closure. Moreover, the Y216 residue (critically involved in K^+ binding) interacts with VU0463271 through one hydrogen bond with the phenyl-3-pyridazinyl group. This creates steric hindrance along the ion-permeation pathway. The fact that VU0463271-KCC1 is the only CCC structure solved in the OO conformation, together with the fact that KCC1 IO conformation was solved without VU0463271, suggests that VU0463271 may stabilize the OO conformation of KCC1. Comparing KCC1 IO and OO states, one can detect the positional shift of TM3, TM4, TM8, TM9, TM10, which regulates the extracellular gate (for the entry of Cl^- and K^+ to the binding sites, in proximity to TM1 and TM6) and occlusion of the intracellular gate. However, the solution of the KCC1-VU0463271 complex was obtained without K^+ in the buffer. Thus, the question of substrate/inhibitor competition for binding remains unresolved. Moreover, in cell line-based experiments, the potency of VU0463271 decreases when the uptake of thallium or rubidium (K^+ congeners: chemical species that share similar physico-chemical properties) increases [111]. VU0463271 also interacts with the conserved M215 residue, located on TM3 adjacent to Y216, mutation of which decreases VU0463271 binding affinity by ~65-fold. Importantly, mutation of this residue in NKCC1 (M382) decreases the binding affinity of a loop-diuretic inhibitor bumetanide, suggesting a similar binding site for the respective targets of VU0463271 and bumetanide, namely *h*KCC1 and *h*NKCC1 [13]. As for bumetanide, mutations in NKCC1 located on one side of TM3 (Y383, M382, A379, N376, A375, F372, G369, I368) decrease loop-diuretic inhibitor and ion affinity. Moreover, the A483C mutant in *r*NKCC1 (A493 in *h*NKCC1), part of the flexible and discontinuous helix TM6a and close to the Cl^--binding site, shows a sixfold increase in bumetanide affinity, with little or no change in ion affinities [123]. Studies indicating small-molecule biding sites are key to structure-based drug discovery programs to design new therapeutic approaches for the pathologies associated with mutations in CCC transporters (Figure IB).

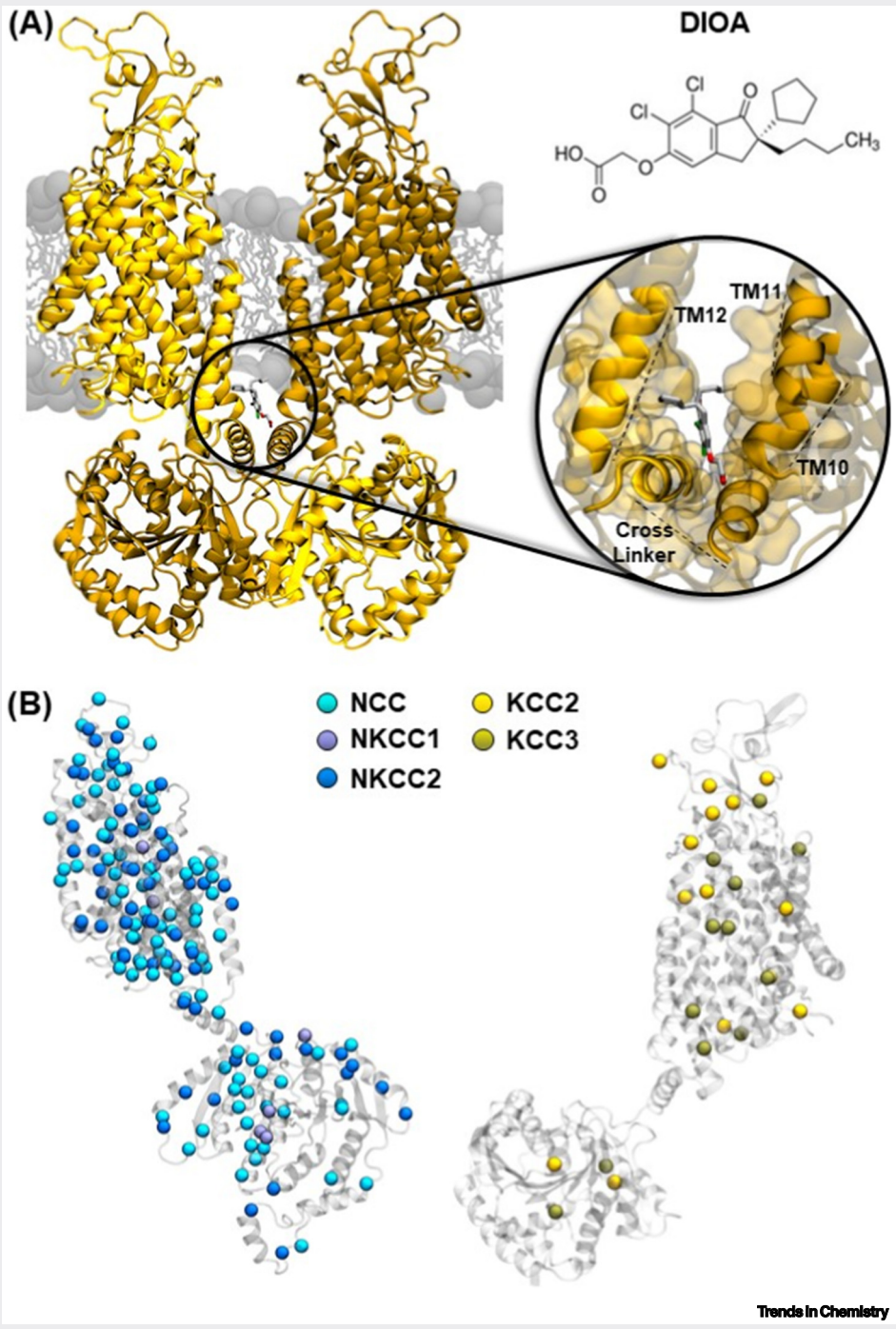

Figure I. Binding site in KCC3 for the small-molecule dihydroindenyl-oxy acetic acid (DIOA) and human disorders linked to cation-coupled chloride cotransporters (CCCs). (A) Representation of the transmembrane (TM) and the C terminal (CT) domains of *h*KCC3, with the inhibitor DIOA bound in the central cleft, and solved by cryogenic electron microscopy [Protein Data Bank (PDB) code: 6M22]. The magnified area shows the DIOA-binding site in the dimeric interface, formed by TM11, TM12, and the crosslinker helices of both monomers. (B) Left. TM domain of *h*NKCC1 (PDB code: 6PZT) and CT domain of *Dr*NKCC1 (PDB code: 6NPL). Spheres represent residues that are associated with human pathologies, when mutated. Light, medium, and dark blue represent residues identified in NCC, NKCC1, and NKCC2, respectively. To map mutations from *h*NCC and *h*NKCC2 on the *h*NKCC1 TM domain structure, sequence alignments were performed using BLAST. The mutated residue's positions were extrapolated from their original sequence and aligned to NKCC1 sequence and structure. This same procedure was followed to map mutations from human NCC, NKCC1, and NKCC2 on *Dr*NKCC1 CT domain structure. Right. TM and CT domains of *h*KCC3 (PDB code: 7D90). Light and dark yellow spheres represent pathological mutations identified in *h*KCC2 and *h*KCC3, respectively. The *h*KCC2 protein sequence was aligned to *h*KCC3 sequence and mutations for both *h*KCC2 and *h*KCC3 were mapped onto the superimposed structure.

of NCC increased transport affinity or impaired membrane localization [50,51]. Moreover, in the EC domain of *h*KCC2 and *m*KCC4, mutation of glycosylation sites and close residues prevented protein glycosylation and drastically reduced the transporter activity and membrane expression [15,27,52].

Table 2. Amino acid residues involved in post-translational modifications (PTMs)

CCC	PTM sites	Possible effect on expression, trafficking, and function	Refs
NCC	T46, T55, T60	T58 (rat, T60 h): dephosphorylation (PP4) inhibits activity but does not affect membrane trafficking, activation by phosphorylation (WNK3); T46, T55, T60: activation by phosphorylation (WNK1), T60A inhibits phosphorylation also of T46 and T55	[49]
	N404, N424	Membrane localization is impaired, increased Cl transport affinity and thiazide affinity	[50]
NKCC1	RVXFXD (107–112 in shark)	Dephosphorylation (PP1) activity modulation	[45,47]
	Shark: T184, T189, T202, (h: T212, T217, T230), shark: T175, T179, T184 (h: T203, T207, T212)	Activation by phosphorylation, T203, T207, T212: WNK3 phosphorylation activation	[35,43,46]
NKCC2	S91, T95, T96, T100, T101, T105, T111, S130	Activation by phosphorylation, T96, T101, T111: making NKCC2 not responsive to low Cl	[41,42]
KCC1	T5, T1048	Inhibitory phosphorylation	[34,44]
	N312, N361	Glycosylation sites	[21]
KCC2	N283, N291, N310, L311H, N328, N338, N339	Glycosylation sites, L311H: decreases KCC2 glycosylation, membrane expression, and transport activity, EIMFS	[15,51]
	T6, S25, S26, S31, T34, Y903, T906, S913, T929, S937, S940, S988, T999, T1007, S1022, S1025, S1026, T1029, T1048, Y1087	T6, T906, T1007, T1048: inhibitory phosphorylation, Y903, Y1087: phosphorylation reduces KCC2 membrane stability, Y1087D reduces its activity, NO affecting protein expression, S940: phosphorylation stimulates membrane expression and transport activity	[26,34,37,40,44,52]
KCC3	T5, S29, S32, S50, S96, S148, T991, S1032, T1048, S1064	Inhibitory phosphorylation, T991, T1048: Cl-sensitive WNK3 phosphorylation inhibition, T991A/T1048A constitutively active cotransport; T991A linked to early onset, progressive, and severe peripheral neuropathy	[26,34,44]
	S45E/T940E/T997E, S45A/T940V/T997V	Resemble phosphorylated (S45E/T940E/T997E) & dephosphorylated (S45A/T940V/T997V) states	[28]
KCC4	T6, T1048	Inhibitory phosphorylation	[34,44]
	N312, N331, N344, N360	Triple (N312/331/344/Q) and quadruple (N312/331/344/360/Q) mutations accumulate in the endoplasmic reticulum, affecting membrane trafficking and protein expression. Mutations of N331Q/N344Q inhibit the membrane trafficking. N312Q prevents glycosylation and drastically reduces KCC4 activity.	[27,48]

Ubiquitination is less studied among the post-translational modifications of CCCs. However, several ubiquitination sites have been characterized for NCC. Interestingly, ubiquitination can directly modulate NCC transporter function, endocytosis, and degradation. Moreover, ubiquitination can also indirectly affect the membrane expression of NCC through the degradation of kinases involved in its phosphorylation [53]. Nevertheless, it is still unknown what precise ubiquitination sites are responsible for the specific ubiquitination-dependent NCC changes.

CCC mutations associated with human diseases

CCC mutations (e.g., missense, deletions, nonsense, frameshift, altered splice site) associated with human diseases result in changes in the amino acid sequence of CCCs, prevalently at the level of the TM domain, with some also involving residues in the NT and CT domains (Box 2). These mutations affect CCC protein synthesis (e.g., truncated or differently spliced proteins), processing, membrane insertion, function, and internalization (Table 3).

Nearly 200 mutations in the *SLC12A3* gene, which encodes for NCC, are linked to Gitelman syndrome (GS) [50,54]. GS is an inherited renal disorder characterized by hypokalemia, metabolic alkalosis, hypocalcemia, urinary calcium, and hypomagnesaemia. The mutations linked to GS are

Table 3. Mutations linked to human diseases and expression/trafficking/activity changes

CCC	Mutation	Domain	Linked disease	Effect on expression, localization, and activity	Refs
NCC	T60M, D62N/H, R83Q, Q95R, E121D	NT	GS	E121D: membrane localization not affected. ↓ Thiazide-sensitive Na uptake	[49,54,57]
	R145C, I154F, L157P, R158Q/L, T163M, W172R, S178L, T180K, G186D, I192T, T194I, G196V, R209W, R209Q, L215P, A226T, T235R, D259N, R261H, G264A, L272P, M279R, S283Y, K284R, A285G, T304M, T304P,A313V, S314F, G316V, R321W, R334W, T339I, R339C, G342X, P349L, S350L, N359K, G362S, G374V, Y386C, T392I, R399C, R399P, S402X, S402F/R209W, N406H, C421R,N426K, C430G, G439S, G439V, N442S, A459D, G463E, A464T, S475C, K478E, C484W, D486N, Y489H, G496C, A523T, N534S, L542P, F545L, S555L, P560R, P560H, A569V, L571P, D566K, A569E, A570V, L571P,V578M, M581L, A588V	TM	GS	T392I, N442S, S475C, Y489H: ↓ Thiazide-sensitive Na uptake. T392I, N442S: membrane localization impaired. S475C, Y489H: membrane localization not affected.	[49,54,55,57]
	H234Q		Salt-losing tubulopathy		[59]
	(r)L153F, (r)S186F, (r)A230T, (r)F493L		Low blood pressure	↓ Na uptake activity, S186F ↓ Protein expression	[60]
	R604Q, N611S, G613S, S615L, N617R, L623P, G630V, H637Y, R642G, P643L, V647M, T649M, R655L, R655C, R655H, V659M, L671P, M672I, V677M, L700P, S710X, Q722X, A728T, G729V, G731R, P735R, L738R, G741R, P751L, S833T, L849H, L850P, L858F, L858H, L859P, R861C, R871H, M881T, R896Q, R913Q, R913N, R919C, R928C, E941X, K957X, N958K, R955Q, N958K, R968X, T1026I, Q1030A	CT	GS	P751L: membrane localization not affected. ↓ Thiazide-sensitive Na uptake, N958K: impaired Na transport & ↑ endoplasmic reticulum stress activation, Q1030A: membrane localization impaired. ↓ Thiazide-sensitive Na uptake	[49,54,56,57,58]
	N640S, T649M, L892P, P947S		Salt-losing tubulopathy		[59]
	(r)G777E		Low blood pressure	↓ Na uptake activity, No change in membrane expression	[60]
	A728T, R904Q, R919C		Hypertension	R919C: membrane expression not affected. ↑ Na uptake	[49]
NKCC1	H186AfsX17	NT	NDD &/or cochleovestibular defect	↓ K transport activity	[63]
	Y199C		SCZ	↑ Cl-dependent & bumetanide-sensitive activity even in hypotonicity	[64]
	A327V, N376I, A379L, R410Q	TM	NDD &/or cochleovestibular defect	↓ K transport activity	[63]
	W892X, E980K	CT	NDD &/or cochleovestibular defect	↓ K transport activity	[63]
	E979K, D981Y, P988T		Hearing loss		[62]
	V1026FfsXX		multisystem impairment		[12]
NKCC2	V9fs, W179R, R199C, W202C	NT	Blood pressure variation		[73]
	D12fs, R116H		Hypokalemic disorders		[81]
	G193R,		Salt-losing tubulopathy		[80]

Table 3. (continued)

CCC	Mutation	Domain	Linked disease	Effect on expression, localization, and activity	Refs
	V9fs, D12fs, R116H, N117X, L184Q, M195fs, V204A		BS		[72]
	E113dup, F177Y, G193R, L196P, R199G, G224D		Antenatal/neonatal BS	F177Y: ↓ half ion transport activity, G193R: membrane expression & localization not affected. Loss ion transport activity.	[75,76,79]
	A244D, G257S, V272F, D296A, R302GfsX2, R302fs, P348QfsX3, K354NfsX73, G397A, A435V, C436Y, C461R, L463S, R471X, G493AfsX53, L495PfsX49, A498V, A508_S511del, S507P, A508T, L522fs, P544S, A555T, A555V, L560P, F611L, D648N, G652S	TM	BS		[71,72]
	G243E, A267S, R302Q, G319R, A337V, P348QfsX3, E368G, C436S, C436Y, G443R, G478A, G478R, A508T, A510D, N526del, Y538X, F611L, W625X, A628D		Antenatal/neonatal BS	G319R, A508T: membrane expression & localization not affected. Loss ion transport activity. A267S: ↓ expression, functionally impaired transporter, N326 del: ↓ expression, functionally impaired transporter	[75,76,78,79]
	Y245del, R302fs, L522fs		Hypokalemic disorders		[81]
	Y245fs, F380fs, A508T, F611fs, A628D		Neonatal hyperparathyroidism		[77]
	R302W		Salt-losing tubulopathy		[80]
	G257S, G478R, N526del, A555T, G612R, G652S, Q656X		Blood pressure variation		[73]
	(r)T231M, (r)R298W, (r)N395S, (r)L501V, (r)P565H			↓ Na uptake, no change in protein expression, (r)N395S: ↑ Na uptake activity, no change in protein expression	[60]
	D699N, D699fs, K706RfsX23, K741X, F747fs, D792fsX4, G809V, Q823fs, R833IfsX15, W915X, D918fs, G921V, N984fsX26	CT	BS		[71,72]
	K706RfsX23, R761X, G920E, Y998X, D918fs		Antenatal/neonatal BS	Y998X: membrane expression & localization not affected. Loss ion transport activity.	[74,76,79]
	D699fs, W936X		Salt-losing tubulopathy		[80]
	R833Ifs, T931fsX10		Neonatal hyperparathyroidism		[77]
	F747fs, E832A		Blood pressure variation		[73]
	(r)Y1066C, (r)P1079A			↓ Na uptake, no change in protein expression	[60]
KCC2	E50_Q93del	NT	EIMFS	Impaired Cl extrusion. No change in membrane expression	[88]
	A191V, L288H, L311H, W318S, S323P, S376L, M415V, L403P, L426P, G528D, G551D	TM	EIMFS	A191V: impaired Cl extrusion. No change in membrane expression, L311H: ↓ expression and glycosylation. ↓ Cl extrusion activity S323P, M415V: impaired Cl extrusion. No change in membrane expression, L426P, G551D: ↓ expression and glycosylation. Loss Cl extrusion activity	[51,88]

(continued on next page)

Table 3. (continued)

CCC	Mutation	Domain	Linked disease	Effect on expression, localization, and activity	Refs
	V473I		IGE		[89]
	S748del, R857L	CT	EIMFS		[87,88]
	R1048W		ASD		[90]
	R952H, R1049C		ASD, SCZ, IGE	Impaired transport activity	[85,90]
	R952H		Febrile seizures	↓ Cl extrusion. Impaired ability to form dendritic spines. ↓ Surface expression	[86]
KCC3	Y192SfsX	TM	AS	Slower nerve conduction	[101]
	R207C, I301SfsX, F493CfsX		ACC	Reduced myelinated fibers	[102]
	P373SplicX42, F529X, G539D, R675X		ACCPN		[102,103]
	P605L		Congenital hydrocephalus & ACC	Membrane expression not affected. ↓ K transport.	[105]
	Y678LfsX		ACC		[102]
	T991A	CT	PN	↓ Phosphorylation. Constitutive activity	[100]
	T813X, R1011X		ACCPN	T813X: membrane expression & glycosylation not affected. Loss K transport activity	[103]

predominately located in the ion-translocation pathway, the EC domain, the TM–TM and TM–cytosol interfaces, and the NT and CT domains, likely affecting NCC folding and stability [20,55,56]. *In vitro* functional characterization of NCC missense mutations associated with GS revealed defective NCC plasma membrane expression, localization, and activity [57,58]. Interestingly, some NCC mutations associated with GS are also associated with salt-losing tubulopathy [59]. Other NCC mutations are linked to hypertension/increased Na^+ transport or reduction of blood pressure/Na^+ uptake [50,60]. NCC knockout (KO) mice are healthy, fertile, and grow normally, despite GS-like symptoms [61].

Mutations in the *SLC12A2* gene, which encodes for NKCC1, are associated with hearing, brain, and multiorgan disorders [12,62–64]. For example, mutations within the NKCC1 sequence have been found in patients affected by neurodevelopmental disorders (NDD) and/or bilateral non-syndromic sensorineural hearing loss. All these mutations decrease K^+ transport *in vitro* [63]. A detected 22-kb homozygous deletion in NKCC1 is associated with Kilquist syndrome, a syndromic sensorineural hearing loss characterized by the absence of saliva, tears, and mucus release, and by respiratory/gastrointestinal problems [65,66]. Moreover, a *de novo*, loss-of-function mutation leading to a frameshift and truncation of NKCC1 CT domain has been linked to multiorgan impairment in vascular, pulmonary, gastrointestinal, and urinary tissues [12]. NKCC1 KO mice die postnatally due to growth retardation, difficulties in maintaining balance, and reduced blood pressure [67,68]. They also develop inner ear dysfunction and deafness, male infertility, salivation impairment, and nervous system deficits (hyperexcitability and impaired pain perception) [1,69]. Notably, altered NKCC1 expression has been described in patients and mouse models of Down syndrome, schizophrenia (SCZ), temporal lobe epilepsy (TLE), and Huntington disease [70].

More than 80 mutations of the *SLC12A1* gene, which encodes for NKCC2, have been associated with Bartter syndrome (BS) type 1, a renal disorder characterized by polyuria, renal tubular hypokalemic alkalosis, hypercalciuria [71,72], and blood pressure alterations [60,73]. Other mutations in the NKCC2 TM and CT domains in antenatal/neonatal BS patients are associated with

premature delivery, polyhydramnios, nephrocalcinosis, and hyperthyroidism [74–78]. Some of these mutations have been studied *in vitro*, showing low expression profile and lack of Na^+ transport [79]. Other mutations in TM and CT or NT domains have been linked to salt-losing tubulopathy or hypokalemic disorders, respectively [80,81]. NKCC2 KO mice exhibit BS-like symptoms that do not allow pups to survive [82].

No specific human disorders have been linked to mutations in the *SLC12A4* gene, which encodes for KCC1. Nevertheless, KCC1 is relevant in hematopoietic lineage and cancer development [83]. KCC1 KO mice are similar to their WT littermates in terms of body weight, histological examination of organs, auditory system, and seizure susceptibility [84].

Mutations in the *SLC12A5* gene, which encodes for KCC2, have been found in subjects affected by brain disorders. In particular, most patients with KCC2 mutation have some form of epilepsy, such as epilepsy of infancy with migrating focal seizures (EIMFS), febrile seizures, or idiopathic generalized epilepsy (IGE) [52,85–89]. Interestingly, R952H or R1049C point mutations, found in patients with epilepsy, are also associated with SCZ or autism spectrum disorder (ASD) [85,86,90]. Another mutation (R1048W) is also associated with ASD [90]. All these KCC2 mutants reduce expression, trafficking, and/or glycosylation and Cl^- extrusion activity [52,85,86,88,90]. KCC2 full-KO mice die immediately after birth due to motor deficits and respiration failure [91]. Isoform KCC2b KO mouse are viable for up to 2 weeks and have generalized seizures [92,93]. Mice with mutations at KCC2 CT domain phosphorylation sites (preventing KCC2 phosphorylation) or constitutively KCC2 dephosphorylated mice (S940A, T906A, and T1007A) display impairment of KCC2 activity and are good models of neurodevelopmental diseases, social/cognitive impairment, and status epilepticus, in line with human data [94–96]. Mice expressing phosphomimetic KCC2 mutations (T906E-T1007E) have altered Cl^- extrusion, which leads to early death, locomotor impairment, touch-evoked status epilepticus, and altered neuronal inhibition [36,97]. Notably, altered KCC2 expression has been described in patients with and/or mouse models of ASD, SCZ, TLE, Huntington disease, and Rett syndrome [98].

Mutations in the *SLC12A6* gene that encodes for KCC3 have been found in subjects with agenesis of corpus callosum (ACC) with peripheral neuropathy (PN) and Andermann syndrome (AS), an early onset PN associated with various degrees of mental disability, psychotic symptoms, and ACCPN [99–103]. In particular, T813X is the predominant KCC3 variant associated with ACCPN. T813X is correctly expressed and glycosylated, but loses K^+ transport activity [103]. Moreover, T991A associated with early onset and progressive PN abolishes KCC3 phosphorylation, resulting in constitutively active transporter and altered cell volume homeostasis [100]. Rare KCC3 variants have been found in bipolar disorder patients [104]. Finally, the P605L mutation, which leads to impaired K^+ transport, has been identified in people affected by congenital hydrocephalus and ACC, but no PN [105]. KCC3 KO mice display deafness, reduced seizure threshold, neurogenic hypertension, and locomotor dysfunction, which resembles AS [103,106].

Only a *de novo* 2.6-kb copy number deletion in KCC4-encoding gene (*SLC12A7*) was recently identified in a family affected by sporadic congenital hydrocephalus [105]. KCC4 KO mice develop progressive hearing loss until deafness and renal tubular acidosis to compensate for high urinary pH [106].

Implications for CNS drug discovery

CCCs are unselectively targeted by widely used loop and thiazide diuretics to treat mild hypertension, edema, compromised blood pressure, and heart failure [1,2]. CCCs have also been most recently implicated in neuronal pathophysiology and cancer biology [3,107]. These diseases all

involve gene mutations (Table 3) or defective expression of CCCs [48,98]. The same CCCs are sometimes involved in multiple disorders, raising the possibility of treating them all with the same drug. For example, the unselective NKCC inhibitor and diuretic drug bumetanide has been repurposed with positive outcomes in clinical trials and case studies to treat brain disorders in patients (e.g., ASD, SCZ, TLE, neonatal seizures, Parkinson's disease) [108]. Accordingly, up-regulation of NKCC1 and/or downregulation of KCC2 have been described in brain samples of patients and animal models of several brain disorders [70,98]. However, bumetanide's strong diuretic effect, mostly due to NKCC2 inhibition, jeopardizes treatment compliance and creates safety issues for the chronic treatment required for brain disorders [70,109]. Thus, recent efforts have sought to develop NKCC1-specific antagonists and new KCC2 agonists [110–112].

In this context, the recent structural information on CCCs creates the possibility of the structure-based design of new and selective CCC modulators. For example, combined with information from mutagenesis and chimeric protein studies, these structures suggest targeting of the TM domain, and also of specific residues at the CT and NT domains, which impact CCC sensitivity to ligands [20,24,25]. Since the EC loops in NCC and NKCCs have different amino acid sequences (despite a conserved structural motif), these loops could be a potential target for isoform-specific drugs. Moreover, the NT domain is poorly conserved among the diverse CCCs, which could favor the development of selective drugs for the diverse CCCs. Finally, chemical interventions to modulate kinase pathways could interfere with CT domain phosphorylation and thus with regulation of CCCs. Interestingly, this approach could exploit the fact that WNKs can modulate CCCs in opposite directions. Inhibiting WNKs could be especially important in the diverse brain disorders characterized by increased intracellular Cl^- homeostasis. Indeed, in neurons, NKCC1 functions as a Cl^- importer, whereas KCC2 functions as a Cl^- exporter. Similarly, glycosylation (at the EC domain) or ubiquitination (at NT and CT domains) could also be considered to modulate CCC activity for therapeutic approaches. For example, targeting upstream glycosidases and/or deubiquitinating enzymes could be one strategy to improve CCC stability and avoid degradation in diseases where mutations of transporters lead to decreased activity [113]. Promoting protein degradation has been a strategy already investigated for other SLC proteins involved, for example, in tumor biology [114] or soluble proteins involved in proteinopathies with accumulation of misfolded or aberrant proteins [115].

Concluding remarks

Our understanding of CCCs has been enriched by their recent cryo-EM structures. These have revealed new chemical and biological insights into the structural topology of CCCs, including the orientation and flexibility of the diverse protein domains, the oligomerization state, and the exact location of ion/ligand-binding sites. This knowledge will stimulate the structure-based drug discovery of potent and selective inhibitors of CCCs. Surprisingly, diuretics are currently the only FDA-approved CCC-targeted drugs on the market and they are all unselective inhibitors. But evidence suggests that it may be possible to modulate specific types and isoforms of CCCs by targeting specific, nonconserved protein domains (see Outstanding questions). This would address many urgent medical needs, given the wide range of pathologies in which CCCs are implicated. Further elucidating the structure/function relationship of CCCs will unravel the mechanism for ion transport, leading to a better understanding of the pathophysiology of diverse diseases and innovative, selective, and safe drugs for patients.

Outstanding questions

Mechanism: how many CCCs are yet to be discovered? Under which conditions do CCCs form oligomers in cells? Are monomers and multimers active in the same way in binding/transport mechanism? What protein regulators mediate CCC assembly and depletion/recycle? Are other partner proteins involved in CCC-mediated biological processes? If so, is it possible to modulate CCC activity by targeting these protein interactors?

Detection: how can we design functional assays to screen for and validate CCC functions in cells? Do current antibody-based approaches for CCC detection provide an incomplete picture due to limited accessibility and competition with endogenous proteins? Can we develop detection methods to monitor dynamic CCC-associated processes at high-resolution in living cells?

Diseases: what other diseases will be associated with CCC impairment? Can we develop mapping approaches to detect CCC genome mutations associated with diseases and thus develop early stage biomarkers? Will it be possible to establish suitable CCC-based biomarkers for diagnostic applications?

Ligands: is it possible to selectively target different oligomeric states of CCCs or different CCC isoforms? Will ligands targeting multiple CCCs be beneficial against multifactorial diseases?

Therapies: what disease phenotypes associated with CCC altered function/expression could be treated with pharmacological therapies? Could a single CCC-targeted drug have positive outcomes in many diverse pathologies? Is gene therapy a viable strategy?

Acknowledgments

We acknowledge Dr Pietro Vidossich (IIT, Genoa, Italy) and Dr Ming Zhou (Baylor College of Medicine, Houston, USA) for constructive comments, helpful discussions, and critical reading of the manuscript. This work was supported by funding from the European Union's Horizon 2020 research and innovation programme under the Marie Skłodowska-Curie (grant

agreement No 843239 to C.P.), Telethon (grant TCP15021 to L.C.), and the European Research Council (ERC) under the European Union's Horizon 2020 Research and Innovation Program (grant agreement no 725563 to L.C.).

Declaration of interests

L.C. is named as co-inventor on the following granted patent: US 9,822,368; EP 3083959; JP 6490077; L.C. is also named as co-inventor on the patent application WO 2018/189225. M.D.V., and L.C. are named as co-inventors on patent application IT 102019000004929.

References

1. Gamba, G. (2005) Molecular physiology and pathophysiology of electroneutral cation-chloride cotransporters. *Physiol. Rev.* 85, 423–493
2. Bazua-Valenti, S. *et al.* (2016) Physiological role of SLC12 family members in the kidney. *Am. J. Physiol. Renal Physiol.* 311, F131–F144
3. Kaila, K. *et al.* (2014) Cation-chloride cotransporters in neuronal development, plasticity and disease. *Nat. Rev. Neurosci.* 15, 637–654
4. Payne, J.A. *et al.* (2003) Cation-chloride co-transporters in neuronal communication, development and trauma. *Trends Neurosci.* 26, 199–206
5. Starremans, P.G. *et al.* (2003) Dimeric architecture of the human bumetanide-sensitive Na-K-Cl Co-transporter. *J. Am. Soc. Nephrol.* 14, 3039–3046
6. Monette, M.Y. and Forbush, B. (2012) Regulatory activation is accompanied by movement in the C terminus of the Na-K-Cl cotransporter (NKCC1). *J. Biol. Chem.* 287, 2210–2220
7. Uvarov, P. *et al.* (2009) Coexpression and heteromerization of two neuronal K-Cl cotransporter isoforms in neonatal brain. *J. Biol. Chem.* 284, 13696–13704
8. Yamashita, A. *et al.* (2005) Crystal structure of a bacterial homologue of Na+/Cl−dependent neurotransmitter transporters. *Nature* 437, 215–223
9. Kahle, K.T. *et al.* (2010) Phosphoregulation of the Na-K-2Cl and K-Cl cotransporters by the WNK kinases. *Biochim. Biophys. Acta* 1802, 1150–1158
10. Morita, Y. *et al.* (2014) Characteristics of the cation cotransporter NKCC1 in human brain: alternate transcripts, expression in development, and potential relationships to brain function and schizophrenia. *J. Neurosci.* 34, 4929–4940
11. Isenring, P. and Forbush, B. (2001) Ion transport and ligand binding by the Na-K-Cl cotransporter, structure-function studies. *Comp. Biochem. Physiol. A Mol. Integr. Physiol.* 130, 487–497
12. Delpire, E. *et al.* (2016) A patient with multisystem dysfunction carries a truncation mutation in human SLC12A2, the gene encoding the Na-K-2Cl cotransporter, NKCC1. *Cold Spring Harb. Mol. Case Stud.* 2, a001289
13. Somasekharan, S. *et al.* (2012) Loop diuretic and ion-binding residues revealed by scanning mutagenesis of transmembrane helix 3 (TM3) of Na-K-Cl cotransporter (NKCC1). *J. Biol. Chem.* 287, 17308–17317
14. Warmuth, S. *et al.* (2009) X-ray structure of the C-terminal domain of a prokaryotic cation-chloride cotransporter. *Structure* 17, 538–546
15. Agez, M. *et al.* (2017) Molecular architecture of potassium chloride co-transporter KCC2. *Sci. Rep.* 7, 16452
16. de Jong, J.C. *et al.* (2003) The structural unit of the thiazide-sensitive NaCl cotransporter is a homodimer. *J. Biol. Chem.* 278, 24302–24307
17. Bai, X. *et al.* (2017) Structural biology of solute carrier (SLC) membrane transport proteins. *Mol. Membr. Biol.* 34, 1–32
18. Lytle, C. *et al.* (1998) A model of Na-K-2Cl cotransport based on ordered ion binding and glide symmetry. *Am. J. Phys.* 274, C299–C309
19. Krishnamurthy, H. *et al.* (2009) Unlocking the molecular secrets of sodium-coupled transporters. *Nature* 459, 347–355
20. Chew, T.A. *et al.* (2019) Structure and mechanism of the cation-chloride cotransporter NKCC1. *Nature* 572, 488–492
21. Liu, S. *et al.* (2019) Cryo-EM structures of the human cation-chloride cotransporter KCC1. *Science* 366, 505–508
22. Yang, X. *et al.* (2020) Structure of the human cation-chloride cotransporter NKCC1 determined by single-particle electron cryo-microscopy. *Nat. Commun.* 11, 1016
23. Zhao, Y. *et al.* (2020) Inhibitory and transport mechanisms of the human cation-chloride cotransport KCC1. *bioRxiv* Published online July 26, 2020. https://doi.org/10.1101/2020.07.26.221770
24. Xie, Y. *et al.* (2020) Structures and an activation mechanism of human potassium-chloride cotransporters. *Sci. Adv.* 6, eabc5883
25. Chi, X. *et al.* (2021) Cryo-EM structures of the full-length human KCC2 and KCC3 cation-chloride cotransporters. *Cell Res.* 31, 482–484
26. Zhang, S. *et al.* (2021) The structural basis of function and regulation of neuronal cotransporters NKCC1 and KCC2. *Commun. Biol.* 4, 226
27. Reid, M.S. *et al.* (2020) Cryo-EM structure of the potassium-chloride cotransporter KCC4 in lipid nanodiscs. *Elife* 9, e52505
28. Chi, X. *et al.* (2020) Molecular basis for regulation of human potassium chloride cotransporters. *bioRxiv* Published online February 24, 2020. https://doi.org/10.1101/2020.02.22.960815
29. Steffensen, A.B. *et al.* (2018) Cotransporter-mediated water transport underlying cerebrospinal fluid formation. *Nat. Commun.* 9, 2167
30. Shi, Y. (2013) Common folds and transport mechanisms of secondary active transporters. *Annu. Rev. Biophys.* 42, 51–72
31. Krishnamurthy, H. and Gouaux, E. (2012) X-ray structures of LeuT in substrate-free outward-open and apo inward-open states. *Nature* 481, 469–474
32. Monette, M.Y. *et al.* (2011) Rare mutations in the human Na-K-Cl cotransporter (NKCC2) associated with lower blood pressure exhibit impaired processing and transport function. *Am. J. Physiol. Renal. Physiol.* 300, F840–F847
33. Watanabe, M. *et al.* (2009) Clustering of neuronal K+-Cl-cotransporters in lipid rafts by tyrosine phosphorylation. *J. Biol. Chem.* 284, 27980–27988
34. Rinehart, J. *et al.* (2009) Sites of regulated phosphorylation that control K-Cl cotransporter activity. *Cell* 138, 525–536
35. Darman, R.B. and Forbush, B. (2002) A regulatory locus of phosphorylation in the N terminus of the Na-K-Cl cotransporter, NKCC1. *J. Biol. Chem.* 277, 37542–37550
36. Watanabe, M. *et al.* (2019) Developmentally regulated KCC2 phosphorylation is essential for dynamic GABA-mediated inhibition and survival. *Sci. Signal.* 12, eaaw9315
37. Lee, H.H. *et al.* (2010) Tyrosine phosphorylation regulates the membrane trafficking of the potassium chloride co-transporter KCC2. *Mol. Cell. Neurosci.* 45, 173–179
38. Kahle, K.T. *et al.* (2003) WNK4 regulates the balance between renal NaCl reabsorption and K+ secretion. *Nat. Genet.* 35, 372–376
39. Wang, D. *et al.* (2016) WNK3 kinase enhances the sodium chloride cotransporter expression via an ERK 1/2 signaling pathway. *Nephron* 133, 287–295
40. Cordshagen, A. *et al.* (2018) Phosphoregulation of the intracellular termini of K(+)-Cl(-) cotransporter 2 (KCC2) enables flexible control of its activity. *J. Biol. Chem.* 293, 16984–16993
41. Ponce-Coria, J. *et al.* (2008) Regulation of NKCC2 by a chloride-sensing mechanism involving the WNK3 and SPAK kinases. *Proc. Natl. Acad. Sci. U. S. A.* 105, 8458–8463
42. Richardson, C. *et al.* (2011) Regulation of the NKCC2 ion cotransporter by SPAK-OSR1-dependent and -independent pathways. *J. Cell Sci.* 124, 789–800

43. Zhang, J. *et al.* (2016) Functional kinomics establishes a critical node of volume-sensitive cation-Cl(-) cotransporter regulation in the mammalian brain. *Sci. Rep.* 6, 35986
44. de Los Heros, P. *et al.* (2014) The WNK-regulated SPAK/OSR1 kinases directly phosphorylate and inhibit the K+-Cl- co-transporters. *Biochem. J.* 458, 559–573
45. Gagnon, K.B. and Delpire, E. (2010) Multiple pathways for protein phosphatase 1 (PP1) regulation of Na-K-2Cl cotransporter (NKCC1) function: the N-terminal tail of the Na-K-2Cl cotransporter serves as a regulatory scaffold for Ste20-related proline/alanine-rich kinase (SPAK) AND PP1. *J. Biol. Chem.* 285, 14115–14121
46. Vitari, A.C. *et al.* (2006) Functional interactions of the SPAK/OSR1 kinases with their upstream activator WNK1 and downstream substrate NKCC1. *Biochem. J.* 397, 223–231
47. Darman, R.B. *et al.* (2001) Modulation of ion transport by direct targeting of protein phosphatase type 1 to the Na-K-Cl cotransporter. *J. Biol. Chem.* 276, 34359–34362
48. Fukuda, A. and Watanabe, M. (2019) Pathogenic potential of human SLC12A5 variants causing KCC2 dysfunction. *Brain Res.* 1710, 1–7
49. Weng, T.Y. *et al.* (2013) Glycosylation regulates the function and membrane localization of KCC4. *Biochim. Biophys. Acta* 1833, 1133–1146
50. Wang, L. *et al.* (2015) Thiazide-sensitive Na+-Cl- cotransporter: genetic polymorphisms and human diseases. *Acta Biochim. Biophys. Sin. (Shanghai)* 47, 325–334
51. Hoover, R.S. *et al.* (2003) N-Glycosylation at two sites critically alters thiazide binding and activity of the rat thiazide-sensitive Na(+):Cl(-) cotransporter. *J. Am. Soc. Nephrol.* 14, 271–282
52. Stodberg, T. *et al.* (2015) Mutations in SLC12A5 in epilepsy of infancy with migrating focal seizures. *Nat. Commun.* 6, 8038
53. Rosenbaek, L.L. *et al.* (2017) The thiazide sensitive sodium chloride co-transporter NCC is modulated by site-specific ubiquitylation. *Sci. Rep.* 7, 12981
54. Zeng, Y. *et al.* (2019) Genetic analysis of SLC12A3 gene in Chinese patients with Gitelman syndrome. *Med. Sci. Monit.* 25, 5942–5952
55. Fanis, P. *et al.* (2019) A novel heterozygous duplication of the SLC12A3 gene in two Gitelman syndrome pedigrees: indicating a founder effect. *J. Genet.* 98, 1–5
56. De la Cruz-Cano, E. *et al.* (2019) Arg913Gln variation of SLC12A3 gene is associated with diabetic nephropathy in type 2 diabetes and Gitelman syndrome: a systematic review. *BMC Nephrol.* 20, 393
57. Glaudemans, B. *et al.* (2012) Novel NCC mutants and functional analysis in a new cohort of patients with Gitelman syndrome. *Eur. J. Hum. Genet.* 20, 263–270
58. Tang, W. *et al.* (2021) A novel homozygous mutation (p.N958K) of SLC12A3 in Gitelman syndrome is associated with endoplasmic reticulum stress. *J. Endocrinol. Investig.* 44, 471–480
59. Tseng, M.H. *et al.* (2012) Genotype, phenotype, and follow-up in Taiwanese patients with salt-losing tubulopathy associated with SLC12A3 mutation. *J. Clin. Endocrinol. Metab.* 97, E1478–E1482
60. Acuna, R. *et al.* (2011) Rare mutations in SLC12A1 and SLC12A3 protect against hypertension by reducing the activity of renal salt cotransporters. *J. Hypertens.* 29, 475–483
61. Schultheis, P.J. *et al.* (1998) Phenotype resembling Gitelman's syndrome in mice lacking the apical Na+-Cl- cotransporter of the distal convoluted tubule. *J. Biol. Chem.* 273, 29150–29155
62. Mutai, H. *et al.* (2020) Variants encoding a restricted carboxy-terminal domain of SLC12A2 cause hereditary hearing loss in humans. *PLoS Genet.* 16, e1008643
63. McNeill, A. *et al.* (2020) SLC12A2 variants cause a neurodevelopmental disorder or cochleovestibular defect. *Brain* 143, 2380–2387
64. Merner, N.D. *et al.* (2016) Gain-of-function missense variant in SLC12A2, encoding the bumetanide-sensitive NKCC1 cotransporter, identified in human schizophrenia. *J. Psychiatr. Res.* 77, 22–26
65. Macnamara, E.F. *et al.* (2019) Kilquist syndrome: a novel syndromic hearing loss disorder caused by homozygous deletion of SLC12A2. *Hum. Mutat.* 40, 532–538
66. Koumangoye, R. *et al.* (2020) Novel human NKCC1 mutations cause defects in goblet cell mucus secretion and chronic inflammation. *Cell Mol. Gastroenterol. Hepatol.* 9, 239–255
67. Flagella, M. *et al.* (1999) Mice lacking the basolateral Na-K-2Cl cotransporter have impaired epithelial chloride secretion and are profoundly deaf. *J. Biol. Chem.* 274, 26946–26955
68. Delpire, E. *et al.* (1999) Deafness and imbalance associated with inactivation of the secretory Na-K-2Cl co-transporter. *Nat. Genet.* 22, 192–195
69. Gagnon, K.B. and Delpire, E. (2013) Physiology of SLC12 transporters: lessons from inherited human genetic mutations and genetically engineered mouse knockouts. *Am. J. Physiol. Cell Physiol.* 304, C693–C714
70. Deidda, G. *et al.* (2015) Reversing excitatory GABAAR signaling restores synaptic plasticity and memory in a mouse model of Down syndrome. *Nat. Med.* 21, 318–326
71. Han, Y. *et al.* (2019) Eleven novel SLC12A1 variants and an exonic mutation cause exon skipping in Bartter syndrome type I. *Endocrine* 64, 708–718
72. Sun, M. *et al.* (2017) Genetic heterogeneity in patients with Bartter syndrome type 1. *Mol. Med. Rep.* 15, 581–590
73. Ji, W. *et al.* (2008) Rare independent mutations in renal salt handling genes contribute to blood pressure variation. *Nat. Genet.* 40, 592–599
74. Halperin, D. *et al.* (2019) A novel SLC12A1 mutation in Bedouin kindred with antenatal Bartter syndrome type I. *Ann. Hum. Genet.* 83, 361–366
75. Brochard, K. *et al.* (2009) Phenotype-genotype correlation in antenatal and neonatal variants of Bartter syndrome. *Nephrol. Dial. Transplant.* 24, 1455–1464
76. Pressler, C.A. *et al.* (2006) Late-onset manifestation of antenatal Bartter syndrome as a result of residual function of the mutated renal Na+-K+-2Cl- co-transporter. *J. Am. Soc. Nephrol.* 17, 2136–2142
77. Wongsaengsak, S. *et al.* (2017) A novel SLC12A1 gene mutation associated with hyperparathyroidism, hypercalcemia, nephrogenic diabetes insipidus, and nephrocalcinosis in four patients. *Bone* 97, 121–125
78. Breinbjerg, A. *et al.* (2017) A novel variant in the SLC12A1 gene in two families with antenatal Bartter syndrome. *Acta Paediatr.* 106, 161–167
79. Starremans, P.G. *et al.* (2003) Mutations in the human Na-K-2Cl cotransporter (NKCC2) identified in Bartter syndrome type I consistently result in nonfunctional transporters. *J. Am. Soc. Nephrol.* 14, 1419–1426
80. Nozu, K. *et al.* (2010) The pharmacological characteristics of molecular-based inherited salt-losing tubulopathies. *J. Clin. Endocrinol. Metab.* 95, E511–E518
81. Colussi, G. *et al.* (2007) A thiazide test for the diagnosis of renal tubular hypokalemic disorders. *Clin. J. Am. Soc. Nephrol.* 2, 454–460
82. Takahashi, N. *et al.* (2000) Uncompensated polyuria in a mouse model of Bartter's syndrome. *Proc. Natl. Acad. Sci. U. S. A.* 97, 5434–5439
83. Garneau, A.P. *et al.* (2019) K(+)-Cl(-) cotransporter 1 (KCC1): a housekeeping membrane protein that plays key supplemental roles in hematopoietic and cancer cells. *J. Hematol. Oncol.* 12, 74
84. Rust, M.B. *et al.* (2006) Neurogenic mechanisms contribute to hypertension in mice with disruption of the K-Cl cotransporter KCC3. *Circ. Res.* 98, 549–556
85. Kahle, K.T. *et al.* (2014) Genetically encoded impairment of neuronal KCC2 cotransporter function in human idiopathic generalized epilepsy. *EMBO Rep.* 15, 766–774
86. Puskarjov, M. *et al.* (2014) A variant of KCC2 from patients with febrile seizures impairs neuronal Cl- extrusion and dendritic spine formation. *EMBO Rep.* 15, 723–729
87. Saito, T. *et al.* (2017) A de novo missense mutation in SLC12A5 found in a compound heterozygote patient with epilepsy of infancy with migrating focal seizures. *Clin. Genet.* 92, 654–658
88. Saitsu, H. *et al.* (2016) Impaired neuronal KCC2 function by biallelic SLC12A5 mutations in migrating focal seizures and severe developmental delay. *Sci. Rep.* 6, 30072
89. Till, A. *et al.* (2019) A rare form of ion channel gene mutation identified as underlying cause of generalized epilepsy. *Orv. Hetil.* 160, 835–838

90. Merner, N.D. *et al.* (2015) Regulatory domain or CpG site variation in SLC12A5, encoding the chloride transporter KCC2, in human autism and schizophrenia. *Front. Cell. Neurosci.* 9, 386
91. Hubner, C.A. *et al.* (2001) Disruption of KCC2 reveals an essential role of K-Cl cotransport already in early synaptic inhibition. *Neuron* 30, 515–524
92. Woo, N.S. *et al.* (2002) Hyperexcitability and epilepsy associated with disruption of the mouse neuronal-specific K-Cl cotransporter gene. *Hippocampus* 12, 258–268
93. Blaesse, P. *et al.* (2009) Cation-chloride cotransporters and neuronal function. *Neuron* 61, 820–838
94. Moore, Y.E. *et al.* (2019) Developmental regulation of KCC2 phosphorylation has long-term impacts on cognitive function. *Front. Mol. Neurosci.* 12, 173
95. Kelley, M.R. *et al.* (2016) Compromising KCC2 transporter activity enhances the development of continuous seizure activity. *Neuropharmacology* 108, 103–110
96. Silayeva, L. *et al.* (2015) KCC2 activity is critical in limiting the onset and severity of status epilepticus. *Proc. Natl. Acad. Sci. U. S. A.* 112, 3523–3528
97. Pisella, L.I. *et al.* (2019) Impaired regulation of KCC2 phosphorylation leads to neuronal network dysfunction and neurodevelopmental pathology. *Sci. Signal.* 12, eaay0300
98. Dargaei, Z. *et al.* (2018) Restoring GABAergic inhibition rescues memory deficits in a Huntington's disease mouse model. *Proc. Natl. Acad. Sci. U. S. A.* 115, E1618–E1626
99. Flores, B. *et al.* (2019) A role for KCC3 in maintaining cell volume of peripheral nerve fibers. *Neurochem. Int.* 123, 114–124
100. Kahle, K.T. *et al.* (2016) Peripheral motor neuropathy is associated with defective kinase regulation of the KCC3 cotransporter. *Sci. Signal.* 9, ra77
101. Lourenco, C.M. *et al.* (2012) Expanding the differential diagnosis of inherited neuropathies with non-uniform conduction: Andermann syndrome. *J. Peripher. Nerv. Syst.* 17, 123–127
102. Uyanik, G. *et al.* (2006) Novel truncating and missense mutations of the KCC3 gene associated with Andermann syndrome. *Neurology* 66, 1044–1048
103. Howard, H.C. *et al.* (2002) The K-Cl cotransporter KCC3 is mutant in a severe peripheral neuropathy associated with agenesis of the corpus callosum. *Nat. Genet.* 32, 384–392
104. Meyer, J. *et al.* (2005) Rare variants of the gene encoding the potassium chloride co-transporter 3 are associated with bipolar disorder. *Int. J. Neuropsychopharmacol.* 8, 495–504
105. Jin, S.C. *et al.* (2019) SLC12A ion transporter mutations in sporadic and familial human congenital hydrocephalus. *Mol. Genet. Genomic Med.* 7, e892
106. Boettger, T. *et al.* (2003) Loss of K-Cl co-transporter KCC3 causes deafness, neurodegeneration and reduced seizure threshold. *EMBO J.* 22, 5422–5434
107. Zhou, Y. *et al.* (2017) Discovery of NKCC1 as a potential therapeutic target to inhibit hepatocellular carcinoma cell growth and metastasis. *Oncotarget* 8, 66328–66342
108. Kharod, S.C. *et al.* (2019) Off-label use of bumetanide for brain disorders: an overview. *Front. Neurosci.* 13, 310
109. Lemonnier, E. *et al.* (2012) A randomised controlled trial of bumetanide in the treatment of autism in children. *Transl. Psychiatry* 2, e202
110. Savardi, A. *et al.* (2020) Discovery of a small molecule drug candidate for selective NKCC1 inhibition in brain disorders. *Chem* 6, 2073–2096
111. Delpire, E. *et al.* (2009) Small-molecule screen identifies inhibitors of the neuronal K-Cl cotransporter KCC2. *Proc. Natl. Acad. Sci. U. S. A.* 106, 5383–5388
112. Superti-Furga, G. *et al.* (2020) The RESOLUTE consortium: unlocking SLC transporters for drug discovery. *Nat. Rev. Drug Discov.* 19, 429–430
113. Czuba, L.C. *et al.* (2018) Post-translational modifications of transporters. *Pharmacol. Ther.* 192, 88–99
114. Bensimon, A. *et al.* (2020) Targeted degradation of SLC transporters reveals amenability of multi-pass transmembrane proteins to ligand-induced proteolysis. *Cell Chem. Biol.* 27, 728–739
115. Hanna, J. *et al.* (2019) Protein degradation and the pathologic basis of disease. *Am. J. Pathol.* 189, 94–103
116. Shimamura, T. *et al.* (2010) Molecular basis of alternating access membrane transport by the sodium-hydantoin transporter Mhp1. *Science* 328, 470–473
117. Fang, Y. *et al.* (2009) Structure of a prokaryotic virtual proton pump at 3.2 A resolution. *Nature* 460, 1040–1043
118. Perez, C. *et al.* (2012) Alternating-access mechanism in conformationally asymmetric trimers of the betaine transporter BetP. *Nature* 490, 126–130
119. Shaffer, P.L. *et al.* (2009) Structure and mechanism of a Na+-independent amino acid transporter. *Science* 325, 1010–1014
120. Faham, S. *et al.* (2008) The crystal structure of a sodium galactose transporter reveals mechanistic insights into Na+/sugar symport. *Science* 321, 810–814
121. Tang, L. *et al.* (2010) Crystal structure of the carnitine transporter and insights into the antiport mechanism. *Nat. Struct. Mol. Biol.* 17, 492–496
122. Wahlgren, W.Y. *et al.* (2018) Substrate-bound outward-open structure of a Na(+)-coupled sialic acid symporter reveals a new Na(+) site. *Nat. Commun.* 9, 1753
123. Dehaye, J.P. *et al.* (2003) Identification of a functionally important conformation-sensitive region of the secretory Na+-K+-2Cl- cotransporter (NKCC1). *J. Biol. Chem.* 278, 11811–11817